Inorg. Chem. **2007**, *46*, 6733–6739

Tetrazol-2-yl as a Donor Group for Incorporation of a Spin-Crossover Function Based on Fe(II) Ions into a Coordination Network

Robert Bronisz*

Faculty of Chemistry, University of Wrocław, F. Joliot-Curie 14, 50-383 Wrocław, Poland

Received February 6, 2007

The coordination polymer $\{[Fe(pbtz)_3](ClO_4)_2 \cdot 2EtOH\}_\infty$ (**1**) has been prepared in a reaction between $Fe(ClO_4)_2 \cdot 6H_2O$ and 1,3-di(tetrazol-2-yl)propane (pbtz). The formation of the second product $\{[Fe(pbtz)_3](ClO_4)_2\}_\infty$ (**2**) was also noticed. Both complexes crystallize in the *R*3 space group. The single-crystal X-ray diffraction study of **1** (295, 90 and 230 K) revealed that the 2-substituted tetrazole rings (2tz) coordinate monodentately to the metal ions, forming $Fe(2tz)_6$ cores. There are two crystallographically independent iron(II) ions in **1**. At 295 K the Fe–N4 bond lengths are equal to 2.173(5) and 2.196(5) Å for Fe1 and 2.176(5) and 2.190(4) Å for Fe2. The pbtz ligand molecules act as N4,N4′ connectors, bridging central atoms in the three directions, which leads to the formation of the 3D network. The crystal lattice of **1** is solvated by ethanol molecules. At 295 K the solvent and ligand molecules are disordered. The results of temperature-dependent magnetic susceptibility measurements (5–300 K), and the single-crystal X-ray diffraction studies (90 K) have exhibited that **1** undergoes the thermally induced spin transition HS↔LS (SCO). The $\chi_M T(T)$ dependence shows in the range 200–75 K gradual SCO. Below 75 K the transition is finished and ∼20% of the HS fraction is present in the sample. The HS→LS transition is accompanied by a shortening of the Fe–N bonds of 0.15 Å. At 90 K the ligand molecules are ordered. The presence of **2** in the reaction product was disclosed accidentally, and only the X-ray diffraction studies (250, 90 K) were performed. Also in **2** iron(II) ions serve as topological nodes of the 3D network. Despite the same network topology, **2** crystallizes without ethanol molecules solvating the crystal lattice. The pbtz molecules bridge the neighboring iron(II) ions, coordinating through N4,N4′ atoms of the 2-substituted tetrazole rings forming the $Fe(2tz)_6$ cores. At 250 K the Fe–N bond lengths are equal to 2.208(5) and 2.218(5) Å. In contrast to **1,** the cooling of the crystal of **2** from 250 to 90 K does not involve the shortening of the Fe–N bond lengths. At this temperature, the Fe–N distances remain characteristic for the HS form of the complex and are equal to 2.203(3) and 2.208(3) Å.

Introduction

Construction of the coordination networks using one-pot synthesis demands the use of ligand systems with predefined structures. Such a procedure ensures the presence of all chosen components in the final product. A careful choice of the proper ligand makes possible construction of the networks showing desired features resulting from the combination of structural and physical−chemical properties.[1] However, a tuning of the characteristic of the material, realized for example by the exchange of donor groups, usually influences the structural properties of the ligand molecules. Consequently, modifications can cause changes in the coordination network architecture.[2]

An application of five-membered polyazole rings as donor groups gives the possibility to tune the properties of the ligand molecules both by the careful selection of the polyazole donors and by the type and position of the substituent in the heterocycle ring.[3] Among polyazoles, the 1-substituted, -imidazoles, 1,2,4-triazoles,[4] 1,2,3-triazoles,[5] and tetrazoles,[6] coordinate monodentately, exhibiting a low inclination to the formation of bridges between metal centers. In this group of polyazoles, 1-substituted tetrazole[7,8] and 1-substituted 1,2,3-triazole[5] derivatives occupy the particular

* E-mail: bron@wchuwr.pl.

(1) Kitagawa, S.; Kitaura, R.; Noro, S.-I. *Angew. Chem., Int. Ed.* **2004**, *43*, 2334−2375.
(2) Robin, A. Y.; Fromm, K. M. *Coord. Chem. Rev.* **2006**, *250*, 2127−2157.
(3) Beckmann, U.; Brooker, S. *Coord. Chem. Rev.* **2003**, *245*, 17−29.
(4) Haasnoot, J. G. *Coord. Chem. Rev.* **2000**, *200*−*202*, 131−185.
(5) Bronisz, R. *Inorg. Chem.* **2005**, *44*, 4463−4465.
(6) Gaponik, P. N.; Voitekhovich, S. V.; Ivashkevich, O. A. *Russ. Chem. Rev.* **2006**, *75*, 507−539.

10.1021/ic070223r CCC: $37.00
Published on Web 07/04/2007

position. Their iron(II) complexes show thermal induced spin crossover (SCO). The bispolyazole-type ligands contaning 1-substituted imidazole,[9−17] 1,2,4-triazole,[18−21] and 1,2,3-triazole[5] rings tethered by the alkyl spacer, act as N,N′ connectors forming coordination polymers with various topology and with metal−metal separations dependent on the ligand nature. Di- and tripodal ligands based on 1-substituted tetrazoles exhibit an ability to form the coordination networks as well.[22−26] Similar to the monomeric iron(II) complexes with 1-*R*-tetrazoles, the iron(II) coordination polymers undergo the spin transition.[23−28]

Investigating the coordination properties of 1-, 2-, and 5-substituted tetrazoles, Franke has noticed that the cooling of the $[Fe(2Rtz)_6](ClO_4)_2$ (where 2Rtz is 2-alkyltetrazole) samples is accompanied by the change of color from white to purple.[29] This observation was interpreted as the confirmation of the HS→LS transition. However, at the present time, there is a lack of structurally characterized iron(II) complexes with mono-2-substituted tetrazoles. On the other hand, 2-methyltetrazole in the reactions with Ni(II) ions coordinates monodentately via the N4 nitrogen atom of the tetrazole ring.[30] Such a coordination fashion prompted us to the utilization of 2-substituted tetrazoles as donor groups for the preparation of new family of ligands namely 1,*ω*-di(tetrazol-2-yl)alkanes. Investigations of the coordination properties of 1,*ω*-di(tetrazol-2-yl)alkanes in the reactions with Zn(II) and Cu(II) succeeded in obtaining the coordination polymers. Depending on the alkyl spacer length and reaction conditions, these complexes were isolated as 1D, 2D, and 3D networks.[31−33] Taking into account an extensive structural and spectroscopic similarity of 2-substituted tetrazole complexes in relation to the complexes of 1-substituted regioisomers, we decided to expand the scope of our investigations on the iron(II) complexes, aiming especially at construction of iron(II) SCO coordination polymers. For this purpose, we have examined the properties of 1,3-di(tetrazol-2-yl)propane (pbtz, Scheme 1) in the reaction with iron(II) perchlorate hexahydrate.

Scheme 1

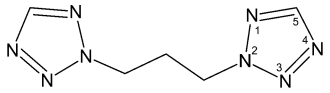

In this paper, the results of variable-temperature magnetic susceptibility measurements and single crystals X-ray diffraction studies of $\{[Fe(pbtz)_3](ClO_4)_2 \cdot 2EtOH\}_\infty$ (**1**), performed at 295 and 230 K for high-spin and at 90K for low-spin forms are presented and discussed. The formation of the second product $\{[Fe(pbtz)_3](ClO_4)_2\}_\infty$ (**2**) crystallizing without ethanol molecules solvating the crystal lattice was noticed unexpectedly. For **2**, which accompanies the formation of **1**, only the X-ray diffraction measurements at 250 and 90 K were performed.

Experimental Section

Material and Methods. Infrared spectra of **1** were recorded with the Bruker IFS66 IR FTIR spectrometer in the range 50−4000 cm^{-1} in nujol mulls. Elemental analyses for carbon, hydrogen, and nitrogen were performed on a Perkin-Elmer 240C analyzer. Temperature measurements of the magnetic susceptibility were carried out with a Quantum Design SQUID magnetometer in the 5−300 K temperature range operating at 1 T. Magnetic data were corrected for the diamagnetic contributions, which were estimated from Pascal's constants. Ethanol was dried by a distillation over a magnesium ethanolate. 1*H*,2,3,4-Tetrazole was prepared using a known procedure.[34] 1,3-Di(tetrazol-2-yl)propane (pbtz) was synthesized in the reaction of 1,3-dibromopropane with sodium tetrazolate according to the procedure described previously.[33] Iron(II) perchlorate hexahydrate purchased from Aldrich was used. The other commercially available reagents were used without further purification. ***Caution!*** *Even though no problems were encountered it is worth mentioning that complexes containing perchlorates are potentially explosive and should be synthesized and handled with care.*

Synthesis of $\{[Fe(pbtz)_3](ClO_4)_2 \cdot 2EtOH\}_\infty$ (1). Synthesis of **1** was performed under nitrogen atmosphere using standard Schlenk techniques. A solution of pbtz (0.6 mmol, 108.8 mg) in absolute

(7) Gütlich, P.; Garcia, Y.; Goodwin, H. A. *Chem. Soc. Rev.* **2000**, *29*, 419−427.
(8) Gütlich, P.; Hauser, A.; Spiering, H. *Angew. Chem., Int. Ed. Engl.* **1994**, *33*, 2024−2054.
(9) Wu, L. P.; Yamagiwa, Y.; Kuroda-Sowa, T.; Kamikawa, T.; Munakata, M. *Inorg. Chim. Acta* **1997**, *256*, 155−159.
(10) Ma, J.-F.; Liu, J.-F.; Xing, Y.; Jia, H.-Q.; Lin, Y.-H. *J. Chem. Soc. Dalton Trans.* **2000**, 2403−2407.
(11) Duncan, P. C. M.; Goodgame, D. M. L.; Menzer, S.; Williams, D. J. *Chem. Commun.* **1996**, 2127−2128.
(12) Tang, L.-F.; Wang, Z.-H.; Chai, J.-F.; Jia, W.-L.; Xu, Y.-M.; Wang, J.-T. *Polyhedron* **2000**, *19*, 1949−1954.
(13) Effendy, Marchetti, F.; Pettinari, C.; Pettinari, R.; Skelton, B. W.; White, A. H. *Inorg. Chem.* **2003**, *42*, 112−117.
(14) Ma, J.-F.; Yang, Y.; Zheng, G.-L.; Li, F.-F.; Liu, J.-F. *Polyhedron* **2004**, *23*, 553−559.
(15) Cui, G.-H.; Li, J.-R.; Tian, J.-L.; Bu, X.-H.; Batten, S. R. *Cryst. Growth Des.* **2005**, *5*, 1775−1780.
(16) Abrahams, B. F.; Hoskins, B. F.; Robson, R.; Slizys, D. A. *CrystEngComm.* **2002**, *4*, 478−482.
(17) Wang, X.-Y.; Li, B.-L.; Zhu, X.; Gao, S. *Eur. J. Inorg. Chem.* **2005**, 3277−3286.
(18) Garcia, Y.; Bravic, G.; Gieck, C.; Chasseau, D.; Tremel, W.; Gütlich, P. *Inorg. Chem.* **2005**, *44*, 9723−9730.
(19) Li, B.; Li, B.; Zhu, X.; Zhu, L.; Zhang, Y. *Acta Crystallogr.* **2003**, *C59*, m350−m351.
(20) Zhao, Q.; Li, H.; Wang, X.; Chen, Z. *New J. Chem.* **2002**, *26*, 1709−1710.
(21) van. Albada, G. A.; Guijt, R. C.; Haasnoot, J. G.; Lutz, M.; Spek, A. L.; Reedijk, J. *Eur. J. Inorg. Chem.* **2000**, 121−126.
(22) van Koningsbruggen, P. J.; Garcia, Y.; Bravic, G.; Chasseau, D.; Kahn, O. *Inorg. Chim. Acta* **2001**, *326*, 101−105.
(23) Schweifer, J.; Weinberger, P.; Mereiter, K.; Boca, M.; Reichl, C.; Wiesinger, G.; Hilscher, G.; van Koningsbruggen, P. J.; Kooijman, H.; Grunert, M.; Linert, W. *Inorg. Chim. Acta* **2002**, *339*, 297−306.
(24) van Koningsbruggen, P. J.; Garcia, Y.; Fournès, L.; Kooijman, H.; Spek, A. L.; Haasnoot, J. G.; Moscovici, J.; Provost, K.; Michalowicz, A.; Renz, F.; Gütlich, P. *Inorg. Chem.* **2000**, *39*, 1891−1900.
(25) van Koningsbruggen, P. J.; Garcia, Y.; Kooijman, H.; Spek, A. L.; Haasnoot, J. G.; Kahn, O.; Linares, J.; Codjovi, E.; Varret, F. J. *Chem. Soc., Dalton Trans.* **2001**, 466−471.
(26) Grunert, C. M.; Schweifer, J.; Weinberger, P.; Linert, W.; Mereiter, K.; Hilscher, G.; Müller, M.; Wiesinger, G.; van Koningsbruggen, P. J. *Inorg. Chem.*, **2004**, *43*, 155−165.
(27) Bronisz, R. Ph.D. Thesis, Wrocław University, Poland, 1999.
(28) Absmeier, A.; Bartel, M.; Carbonera, C.; Jameson, G. N. L.; Weinberger, P.; Caneschi, A.; Mereiter, K.; Letard, J.-F.; Linert, W. *Chem. Eur. J.* **2006**, *12*, 2235−2243.
(29) Franke, P. L. Ph.D. Thesis, Leiden University, the Netherlands, 1982.
(30) van den Heuvel, E. J.; Franke, P. L.; Verschoor, G. C.; Zuur, A. P. *Acta Crystallogr.* **1983**, *C39*, 337−339.
(31) Bronisz, R. *Inorg. Chim. Acta* **2002**, *340*, 215−220.
(32) Bronisz, R. *Inorg. Chim. Acta* **2004**, *357*, 396−404.
(33) Bronisz, R. *Eur. J. Inorg. Chem.* **2004**, 3688−3695.
(34) Kamiya, T.; Saito, Y. *Ger. Offen.*, 2147023, **1973**.

Table 1. Crystallographic Data for **1** (295, 90, 230 K) and **2** (250, 90 K)

	1 (295 K)	**1** (90 K)	**1** (230 K)	**2** (250 K)	**2** (90 K)
empirical formula	$C_{38}H_{54}Cl_4Fe_2N_{48}O_{20}$	$C_{38}H_{54}Cl_4Fe_2N_{48}O_{20}$	$C_{38}H_{54}Cl_4Fe_2N_{48}O_{20}$	$C_{15}H_{24}Cl_2FeN_{24}O_8$	$C_{15}H_{24}Cl_2FeN_{24}O_8$
fw	1756.79	1756.79	1756.79	795.33	795.33
λ (Å)	0.71073	0.71073	0.71073	0.71073	0.71073
space group (No.)	*R*3	*R*3	*R*3	*R*3	*R*3
a (Å)	17.6017(14)	17.2576(8)	17.6018(8)	11.869(3)	11.7898(9)
b (Å)	17.6017(14)	17.2576(8)	17.6018(8)	11.869(3)	11.7898(9)
c (Å)	21.056(2)	20.8493(13)	21.0633(14)	19.284(4)	19.0756(13)
α (°)	90	90	90	90	90
β (°)	90	90	90	90	90
γ (°)	120	120	120	120	120
V (Å^3)	5649.7(8)	5377.5(5)	5651.6(5)	2352.7(9)	2296.3(3)
Z	3	3	3	3	3
D_c (Mg·m^{-3})	1.549	1.627	1.549	1.684	1.725
μ (mm^{-1})	0.624	0.656	0.624	0.735	0.753
R1 ($I > 2\sigma(I)$)[a]	0.0680	0.0520	0.0672	0.0678	0.0440
wR2 ($I > 2\sigma(I)$)[b]	0.2062	0.1437	0.2040	0.1887	0.1108

[a] $R1 = \sum||F_0| - |F_c||/\sum|F_0|$. [b] $wR2 = [\sum w(F_0^2 - F_c^2)^2/\sum w(F_0^2)^2]^{1/2}$.

ethanol (3.0 mL) was added to the solution of $Fe(ClO_4)_2 \cdot 6H_2O$ (0.2 mmol, 72.6 mg) in ethanol (2.5 mL). The resultant clear solution was allowed to stand in a closed Schlenk flask for 1 week at room temperature. After this time, colorless crystals were filtered off and dried in a nitrogen atmosphere. Yield 53% (94.6 mg). Found: C, 25.5; H, 4.20; N, 37.4. Anal. Calcd for $FeC_{15}H_{24}N_{24}Cl_2O_8 \cdot 2EtOH$: C, 25.6; H, 4.52; N, 37.7%. IR: 3519(m, br), 3132(m), 2956(s, sh), 2924(s), 2854(s, sh), 1467(s, sh), 1456(s), 1377(s), 1350(w, sh), 1304(s), 1274(w), 1203(w, sh), 1186(m), 1150(s), 1085(s, br), 1041(s, sh), 989(m), 933(w), 911(w), 880(m), 834(w), 801(w), 764(w), 716(w), 708(w, sh), 701(w, sh), 690(m), 663(w), 624(s)480(m), 481(w), 388(w), 227(w) cm^{-1}.

The single crystal of complex **2** was isolated from the crystalline product accidentally, and only X-ray diffraction studies for this complex were performed.

X-ray Data Collection and Structure Determination. The crystals suitable for X-ray measurements were selected from the crystalline product obtained according to the aforementioned synthesis procedure of the complex. Crystals were coated with a layer of inert oil and immediately transferred to the cold stream of nitrogen of the diffractometer. Crystal data and refinement details for **1** and **2** are listed in Table 1. The measurements of compound **1** were performed at 295 (first crystal sample), 90, and 230 K (second crystal sample). The structure of compound **2** was determined at 250 and 90 K. All measurements of crystals were performed using the Oxford Cryosystem device on Kuma KM4CCD κ-axis diffractometer with graphite-monochromated Mo Kα radiation. The data were corrected for Lorentz and polarization effects. No absorption correction was applied. Data reduction and analysis were carried out with the Oxford Diffraction (Poland) Sp. z o.o. (formerly Kuma Diffraction Wroclaw, Poland) programs. The structures were solved by direct methods (program SHELXS97[35]) and refined by the full-matrix least-squares method on all F^2 data using the SHELXL97[36] program.

In compound **1** at 295 K the carbon atoms C12 and C22 are disordered over two positions with occupancies of 0.88:0.12 and 0.86:0.14, respectively. The bond distances C11′−C12′, C12′−C13′, C21′−C22′, C22′−C23′, and C21−C22 were constrained to 1.52(1) Å. Atoms C12′ and C22′ with the site occupation factors 0.12 and 0.14 were refined isotropically. The rest of the non-hydrogen atoms forming the polymeric macrocation were refined with anisotropic displacement parameters. Both ethanol molecules are disordered also. The ethanol molecule localized on the three-fold axis is disordered over three positions. The second crystallographically independent EtOH molecule is disordered over two positions with occupancy factors of 0.46 and 0.54. For refinement of the respective position of these EtOH molecules, three distance restraints, C−C = 1.44(1) Å, C−O = 1.42(1) Å, and C···O = 2.38(1) Å, were applied.[37] All atoms of both ethanol molecules were refined isotropically. The second ethanol molecule was refined without hydrogen atoms attached to oxygen and carbon atoms. In the ethanol molecule positioned on the three-fold axis and in the pbtz molecules, the hydrogen atoms were placed in geometrically idealized positions and included as riding atoms. One of the two perchlorates was constrained as tetrahedral with Cl−O bonds fixed at 1.44(1) Å and O···O distances restrained to be equal. Atoms from perchlorate anions were refined with anisotropic displacement parameters. At 90 K the propylene chains of both ligand molecules are ordered. At this temperature, all non-hydrogen atoms forming the polymeric skeleton and perchlorate anions were refined anisotropically. Both ethanol molecules remain disordered at this temperature, and the same restraints as at 295 K were applied. The second crystallographically independent ethanol molecule is disordered over two positions with occupancy of 0.72:0.28. Atoms from ethanol molecules were refined isotropically. The second ethanol molecule was refined without hydrogen atoms. The other hydrogens were positioned from the geometry of the ethanol (molecule positioned on the three-fold axis) and pbtz molecules and refined isotropically as riding atoms. At 230 K (heating mode) the same types of restraints were applied as those used in the refinement of the crystal structure at 295 K.

In compound **2** at 250 and 90 K, all non-hydrogen atoms were refined with anisotropic displacement parameters. The idealized positions of the hydrogen atoms were calculated from the geometry of the molecules and refined isotropically as riding atoms.

Results and Discussion

Synthesis and Properties. Complex **1** was prepared in the reaction between pbtz and $Fe(ClO_4)_2 \cdot 6H_2O$ in absolute ethanol in the molar ratio pbtz/Fe(II) = 3:1. Unexpectedly, the occasional formation of complex **2** was also observed. The elementary analysis of the obtained crystalline product stays in agreement with the C, H, and N values expected

(35) Sheldrick, G. M. *SHELXS97, program for solution of crystal structures*; University of Göttingen: Göttingen, Germany, 1997.
(36) Sheldrick, G. M. *SHELXL97, program for crystal structure refinement*; University of Göttingen: Göttingen, Germany, 1997.
(37) Kepert, C. J.; Rosseinsky, M. J. *Chem. Commun.* **1999**, 375−376.

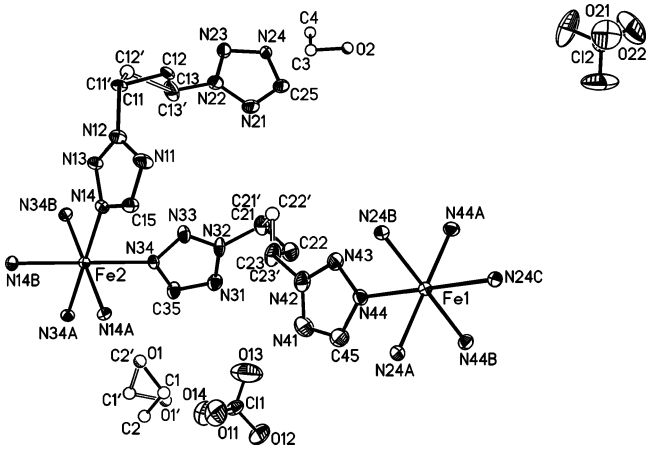

Figure 1. Disordered ligand molecules and coordination environment of Fe(II) ions in **1** at 295 K (thermal elipsoids at the 20% probability level). Hydrogen atoms are omitted for clarity. The alternative positions for the disordered alkyl chains and ethanol molecules are shown by open lines. Selected torsion angles (deg): N12−C11−C12−C13, 68.2(8); C11−C12−C13−N22, 175.0(6); N32−C21−C22−C23, 66(1); C21−C22−C23−N42, 178.7(8); N12−C11′−C12′−C13′, 59(5); C11′−C12′−C13′−N22, 110(3); N32−C21′−C22′−C23′, 58(3); C21′−C22′−C23′−N42, 122(2).

for complex **1**. It shows that compound **2** may occur in the reaction product only in small quantities. A stoichiometry for complex **2** was determined on the basis of the X-ray diffraction studies. Compounds **1** and **2** crystallize as colorless crystals. In contrast to the zinc(II) analogue,[33] **1** is considerably more stable, and in a nitrogen atmosphere, the first symptoms of decomposition (crystals becoming cloudy) arise after a few weeks. On the other hand, complex **1** is hygroscopic. Compound **1** is sensitive to oxidation, and during storage on air, the crystal sample becomes yellowish.

Similarly to the 1-R-tetrazoles and 4-R-1,2,4-triazoles based iron(II) complexes also the cooling of the sample of **1** is accompanied by a pronounced change of color from white to purple indicating the occurrence of the HS→LS transition.

Description of the crystal structure of 1. The crystal of **1** is composed from 3D polymeric macrocations, noncoordinated perchlorate anions and ethanol molecules solvating the crystal lattice. The crystal structure of the investigated iron(II) complex is isomorphic with the structure of $\{[Zn(pbtz)_3](ClO_4)_2 \cdot 2EtOH\}_\infty$.[33]

The X-ray diffraction measurements of **1** were performed at 295, 90, and 230 K (heating mode). This compound crystallizes in the trigonal *R*3 space group. There are two crystallographically independent iron(II) ions. The pbtz ligand molecules coordinate to the metal ions through the N4 nitrogen atoms of the 2-substituted tetrazole rings (Figure 1).

The coordination geometry of both iron(II) ions is slightly distorted octahedral. At 295 K the Fe−N bond lengths are equal to 2.173(5) and 2.196(5) Å for Fe1 and 2.176(5) and 2.190(4) Å for Fe2 (Table 2).

These values are characteristic for the high-spin form of iron(II) ions, and they are similar to that found for complexes with 1-alkyltetrazoles.[23−26,38−40] In compound **1**, one pbtz molecule bridges two iron(II) ions and, simultaneously, the six pbtz molecules are coordinated to the one central atom. Such a bridging fashion of the neighboring iron(II) ions is propagated in the three non-coplanar directions, which leads to the formation of a 3D network (Figure 2).

The differences in the relative orientations of the neighboring octahedrons cause the geometry of the FeN_6 chromophores not to determine the directions of the network propagation. It should be noted that at 295 K the propylene chains of ligand molecules are disordered over two positions

Table 2. Selected Fe−N Distances (Å) and N−Fe−N Angles (deg) for **1** at 295, 230, and 90 K

	295 K	230 K		90 K
Fe1−N24A[a]	2.173(5)	2.187(5)	Fe1−N24A[h]	2.038(4)
Fe1−N44	2.196(5)	2.185(5)	Fe1−N44	2.032(4)
Fe2−N14	2.176(5)	2.192(5)	Fe2−N14	2.045(4)
Fe2−N34	2.190(4)	2.179(5)	Fe2−N34	2.014(4)
N24B[b]−Fe1−N24C[c]	91.4(2)	90.7(2)	N24B[i]−Fe1−N24C[j]	90.7(2)
N24B[b]−Fe1−N44A[d]	89.2(2)	88.9(2)	N24B[i]−Fe1−N44A[k]	88.1(2)
N24B[b]−Fe1−N44	88.8(2)	88.9(2)	N24B[i]−Fe1−N44	89.7(2)
N44B[e]−Fe1−N44	90.6(2)	91.4(2)	N44B[d]−Fe1−N44	91.5(2)
N14−Fe2−N34	89.4(2)	89.5(2)	N14−Fe2−N34	88.8(2)
N14−Fe2−N14A[f]	90.4(2)	90.1(2)	N14−Fe2−N14A[l]	90.8(2)
N14−Fe2−N34B[g]	89.4(2)	89.4(2)	N14−Fe2−N34B[m]	89.4(2)
N34−Fe2−N34A[f]	90.7(2)	91.0(2)	N34−Fe2−N34A[l]	91.0(2)

[a] Symmetry codes: $-1/3 + x, 1/3 + y, 1/3 + z$. [b] Symmetry codes: $2/3 - x + y, 1/3 - x, 1/3 + z$. [c] Symmetry codes: $-1/3 - y, -2/3 + x - y, 1/3 + z$. [d] Symmetry codes: $2 - x + y, 1 - x, z$. [e] Symmetry codes: $-y, x - y, z$. [f] Symmetry codes: $1 - x + y, 1 - x, z$. [g] Symmetry codes: $1 - y, x - y, z$. [h] Symmetry codes: $1/3 + x, 2/3 + y, -1/3 + z$. [i] Symmetry codes: $1/3 - y, -4/3 + x - y, -1/3 + z$. [j] Symmetry codes: $7/3 - x + y, 2/3 - x, -1/3 + z$. [k] Symmetry codes: $1 - y, -1 + x - y, z$. [l] Symmetry codes: $-y, -1 + x - y, z$; *m*: $1 - x + y, -x, z$.

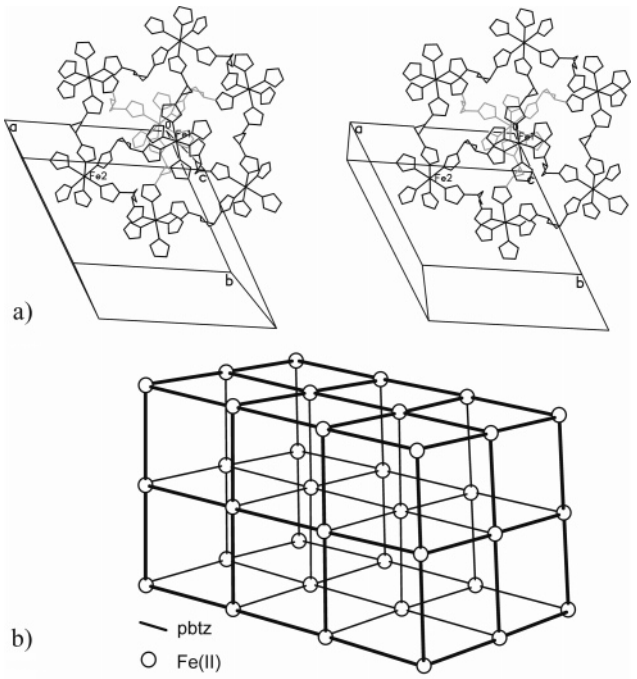

Figure 2. (a) Stereoview of the 3D net in **1** at 295 K. Hydrogen atoms, ethanol molecules, and perchlorate anions are omitted for clarity. (b) A schematic presentation of the 3D network in **1**.

(38) Wiehl, L. *Acta Crystallogr*. **1993**, *B49*, 289−303.

(39) Hinek, R.; Spiering, H.; Sholmeyer, D.; Gütlich, P.; Hauser, A. *Chem. Eur. J.* **1996**, *11*, 1427−1434.

(40) Jeftic, J.; Hinek, R.; Capelli, S. C.; Hauser, A. *Inorg. Chem.* **1997**, *36*, 3080−3087.

in the ratio of ca. 0.88:0.12 and 0.86:0.14. Here both independent pbtz molecules (possessing greater occupation factors) adopt *TG* conformation (N12−C11−C12−C13, 68.2(7)°; C11−C12−C13−N22, 175.0(6)°; N32−C21−C22−C23, 66(1)°; C21−C22−C23−N42, 178.7(8)°) separating iron(II) ions at comparable distances of 10.755(1) and 10.748(1) Å for Fe1−Fe2 and Fe1(x + 1/3, y − 1/3, z − 1/3)−Fe2, respectively. This fitting of the conformation of the ligand molecules to the localization of the coordination sites of the bridged iron(II) ions involves the relative short Fe−Fe distances. It is worth mentioning that the Fe−Fe separations in **1** are shorter at ca. 1.0−3.6 Å than those observed for butyl bispolyazole-based iron(II) coordination polymers exhibiting a discontinuous SCO.[5,26] The counterions are gathered around the $Fe(2tz)_6$ cores. The coordination network is solvated by disordered ethanol molecules. The existence of the O(EtOH)···O(ClO_4^-) and O(EtOH)··· N(tetrazole) contacts (Table S1) between ethanol molecules and perchlorate anions or/and tetrazole rings suggests a presence of intermolecular interactions.

The cooling of the crystal of **1** to 90 K involves significant changes in the crystal structure. At this temperature, the values of appropriate Fe−N bonds lengths are equal to 2.032(4) and 2.038(4) Å for Fe1 and 2.014(4) and 2.045(4) Å for Fe2, respectively (Table 2). This shortening of the Fe−N bond lengths after lowering of the temperature is the characteristic feature of the HS→LS transition in iron(II) complexes. Changes of the Fe−N distances accompanying the complete SCO in the tetrazole-based complexes range usually from ca. 0.16 to 0.20 Å.[23,24,26,41] On the other hand, for incomplete spin transitions, an average decreasing of the Fe−N distance adopts lower values.[42−44] Therefore, the observed shortening of the Fe−N bond lengths in **1** at ca. 0.15 Å for both iron sites may indicate an incomplete SCO. For the majority of the iron(II) SCO complexes, the FeN_6 chromophore adopts geometry that is more regular after the HS→LS transition. In the case of complex **1**, the deformation of the coordination geometry in the HS and LS states are similar. The values of N−Fe−N angles for high spin form vary from 88.8(3)° to 91.4(2)° for Fe1 and from 89.1(2)° to 91.5(2)° for Fe2 and are comparable to that found for low spin species that adopt values of 88.1(2)−90.7(2)° and 88.8(2)−90.8(2)°, respectively. A similar behavior was observed for the other 3D polymeric spin-crossover complex $\{[Fe(btr)_3](ClO_4)_2\}_\infty$ (btr = 4,4′-bi-1,2,4-triazole) where spin transition entails the increasing of the coordination geometry deformation.[45] After the HS→LS transition in **1**, the Fe−Fe separations through ligand molecules are reduced from 10.755(1) to 10.543(1) Å for Fe1−Fe2 and from 10.748(1) to 10.562(1) Å for Fe1(x + 1/3, y − 1/3, z − 1/3)−Fe2. At 90 K all pbtz molecules are ordered and adopt a *TG* conformation. At 90 K, the alcohol molecules remain disordered. The compression of the crystal lattice in **1** brings about a shortening of the intermolecular contacts (Table S1). In the low-spin structure, the number of these interactions practically stays unchanged.

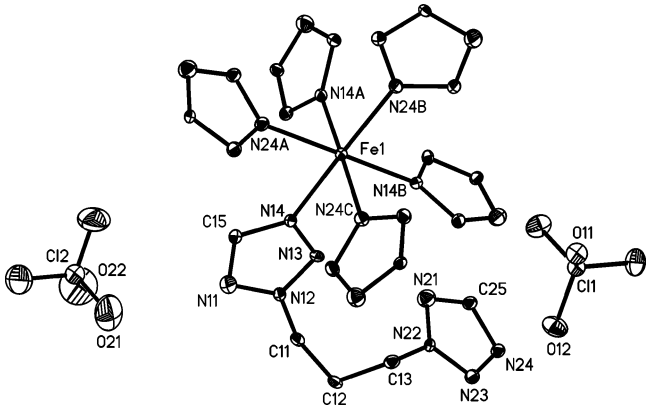

Figure 3. View of **2** showing the coordination environment (thermal elipsoids at the 20% probability level). Hydrogen atoms are omitted for clarity.

After measurement performed at 90K the crystal of **1** was warmed up to 230K and the crystal structure was determined again. At this temperature, the Fe-N4 bond lengths are equal to 2.185(5) for Fe1 and 2.187(5) and 2.179(5) and 2.192(5) Å for Fe2 (Table 2). The values of N4−Fe1-N4 angles range from 88.9(2) to 91.4(2)° and for N4−Fe2-N4 from 89.4(2) to 91.0(2)°. At 230K the Fe−N bond lengths are characteristic for the high spin form of the complex. After LS→HS transition the ligand molecules are disordered. The details concerning the structure of solvent molecules, anions and the scheme of the intermolecular interactions are very similar to these ones observed at 295K. To summarize, the crystal structure of **1** at 230K does not reveal any significant differences in relation to the structure determined at 295K.

Description of the Crystal Structure of 2. For **2**, one single crystal was isolated and the properties of this complex were uncovered only on the basis of the X-ray investigations. Similar to the compound **1**, complex **2** also crystallizes as the 3D coordination polymer. The crystal lattice of **2** is composed of the polymeric macrocation and noncoordinated anions. It is worth underlining that, in contrast to **1**, in the case of complex **2**, there is a lack of the ethanol molecules solvating the crystal lattice.

Complex **2** crystallizes in the *R*3 space group. The iron atom and two perchlorate anions lie on the three-fold axis. The independent part of the unit cell completes one pbtz molecule. Corresponding to the previously described structure of **1** also in this case, the ligand molecule bridges two iron(II) ions coordinating through the N4 and N4′ nitrogen atoms from the 2-substituted tetrazole rings (Figure 3).

In relation to the crystal structure of **1**, a more pronounced distortion of the FeN_6 coordination octahedron in **2** is observed. At 250 K the Fe−N4 bond lengths are equal to 2.208(5) and 2.218(5) Å; the values of N4−Fe−N4 angles range from 87.3(2)° to 94.7(2)° (Table 3).

(41) Kusz, J.; Spiering, H.; Gütlich, P. *J. Appl. Crystallogr.* **2001**, *34*, 229−238.
(42) Real, J. A.; Castro, I.; Bousseksou, A.; Verdaguer, M.; Burriel, M.; Castro, M.; Linares, J.; Varret, F. *Inorg. Chem.* **1997**, *36*, 455−464.
(43) Real, J. A.; Gallois, B.; Granier, T.; Suez-Panamá, F.; Zarembowitch, J. *Inorg. Chem.* **1992**, *31*, 4972−4979.
(44) Guionneau, P.; Létard, J.-F.; Yufit, D. S.; Chasseau, D.; Bravic, G.; Goeta, A. E.; Howard, J. A. K.; Kahn, O. *J. Mater. Chem.* **1999**, *9*, 985−994.
(45) Garcia, Y.; Kahn, O.; Rabarbel, L.; Chansou, B.; Salmon, L.; Tuchagues, J.-P. *Inorg. Chem.* **1999**, *38*, 4663−4670.

Table 3. Selected Fe−N Distances (Å) and N−Fe−N Angles (deg) for **2** at 250 and 90 K

	250 K	90 K
Fe1−N14	2.208(4)	2.207(3)
Fe1−N24	2.218(4)	2.203(3)
N14−Fe−N14A[a]	89.6(2)	90.1(1)
N14−Fe1−N24A[b]	87.3(2)	87.1(1)
N14A[a]−Fe1−N24A[b]	88.3(2)	87.5(1)
N24A[b]−Fe1−N24B[c]	94.7(2)	95.2(1)

[a] Symmetry codes: $-y, x - y, z$. [b] Symmetry codes: $-y + 2/3, x - y + 1/3, z + 1/3$. [c] Symmetry codes: $-x + y - 1/3, -x + 1/3, z + 1/3$.

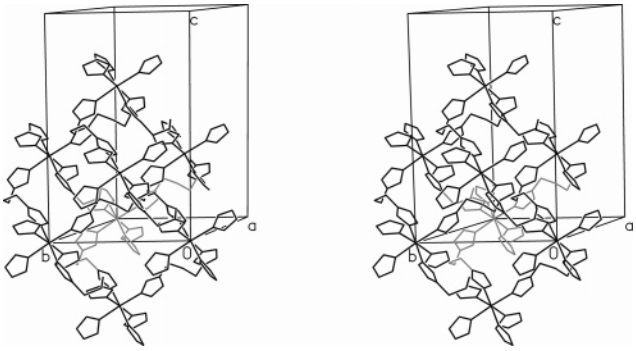

Figure 4. Stereoview of the 3D net in **2** at 250 K. Hydrogen atoms, ethanol molecules, and perchlorate anions are omitted for clarity.

The bridging of the neighboring iron(II) ions occurs in the three directions, which leads to formation of the 3D network (Figure 4).

In compound **2** the topology of the network originates from the coordination geometry of the iron(II) ions, and also here an orientation of the Fe−N bonds is incompatible with the directions of the network propagation. The linkage of the coordination sites of the neighboring Fe(II) octahedrons is realized by the pbtz ligand molecules that adopt the *GG* conformation (N12−C1−C2−C3, 64.1(7)°; C1−C2−C3−N22, 66.3(7)°). Consequently, it forces the significant shortening of the distance between iron(II) ions in comparison with the Fe−Fe separations in **1**. In **2** iron(II) ions are bridged by ligand molecules at distance 9.396(2) Å, i.e., at ca. 1.3 Å shorter than in **1**. The perchlorate anions are ordered and are not engaged in the formation of the hydrogen-bond interactions. In contrast to compound **1**, in the crystal structure of **2** only distant C−H···N and C−H···O contacts are present. The unit cell contains no voids accessible for the solvent molecules.[46]

Unexpectedly, at 90 K no significant differences in relation to the structure of **2** determined at 250 K are observed. The values of Fe−N bond lengths that are equal to 2.203(3) and 2.208(3) Å (Table 3) point to lowering the temperature in the given temperature threshold not involving the change of the spin state of the iron(II) ions. The only observed alteration depends on the small increasing of deformation of the coordination geometry. The values of the N4−Fe−N4 angles range from 87.1(1)° to the 95.2(1)°. The decreasing of the temperature does not involve any differences in the structures of the polymeric macrocation and anions. The weak intermolecular contacts stay unchanged too.

(46) Spek, L. *Acta Crystallogr*. **1990**, *A46*, C34.

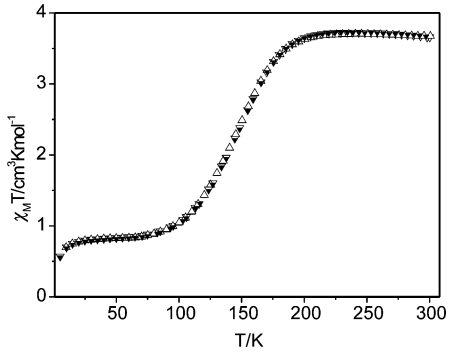

Figure 5. $\chi_M T$ vs T plot for **1** in cooling (▽) and warming (△) modes in the first temperature cycle. For the second cycle, the $\chi_M T$ vs T dependency is depicted using ▼.

Results of Magnetic Susceptibility Measurements of 1. The temperature-dependent magnetic susceptibility measurements for **1** were performed over the 5−300 K range. The magnetic behavior of **1** is shown in Figure 5 in the form of the $\chi_M T$ vs T dependency (χ_M, molar susceptibility; T, temperature).

At 300 K, $\chi_M T$ is equal to 3.66 cm^{3}K/mol which corresponds to the value characteristic for the high-spin form of the iron(II) ion. Upon cooling, the $\chi_M T$ value remains almost constant until 200 K. Further lowering the temperature causes a gradual decrease of $\chi_M T$ that reaches at ca. 75 K the value of 0.87 cm^{3}K/mol. Below 75 K the $\chi_M T$(T) dependency reaches a plateau. It means that ∼20% of the iron(II) ions undergo the HS→LS transition. In the warming mode, the same course of the $\chi_M T$ vs T dependency was noticed as it was observed in the cooling mode. Such behavior indicates an absence of a thermal hysteresis loop. After the sample of **1** was warmed up to 300 K, the second cycle depending on cooling from 300 to 5 K and next heating from 5 to 300 K was performed. No differences in the $\chi_M T$(T) dependency in relation to the first temperature cycle were noticed. The lowering of the $\chi_M T$ value below 10 K may be attributed to the zero-field splitting of the residual high-spin sites.

The presence of the ca. 20% of the paramagnetic fraction stays in agreement with the results of the X-ray diffraction studies. On the other hand, the presence of the second product **2**, which remains in the HS form to 90 K, and the observed facility of the oxidation of **1** may be additional factors responsible for the observed paramagnetism of the sample.

Concluding Remarks

Two iron(II) complexes based on tetrazol-2-yl rings as donor groups are presented in this report. In both compounds neighboring iron(II) ions are bridged by flexible ligand molecules, 1,3-di(tetrazol-2-yl)propane. In these complexes the N4,N4′ single bridging of the neighboring iron(II) ions is propagated in three directions resulting in the formation of the 3D coordination networks. Complex **1** was isolated as the ethanol solvate, whereas **2** crystallizes without ethanol molecules solvating the crystal lattice. The different compositions of **1** and **2** are reflected in the structural details of the polymeric backbones and in the nearest surroundings of the central atoms. The structural dissimilarity of the poly-

meric macrocations results from the ability of the ligand molecules to the adoption of various conformations. In both complexes the differences in the relative orientations of the neighboring iron(II) coordination octahedrons demand a suitable adjustment of the geometry by the bridging pbtz molecules. In **1** and **2** the ligand molecules adopt two different conformations, *TG* or *GG*, respectively. Consequently, in both compounds the central atoms are bridged at various distances, 10.7 or 9.4 Å. It is worth underlining that in spite of differences presented above such bridging of the metal centers leads in both cases to the formation of the topologically identical 3D networks.

Complexes **1** and **2** possess homoleptic surrounding of the metal ions. In both compounds six 2-substituted tetrazole rings coordinating to iron(II) ions via N4 nitrogen atoms form FeN_6 chromophores which has parameters comparable to that found for the iron(II) complexes with 1-substituted regioisomers. The structural consequences initiated by the presence or absence of solvent molecules are also reflected in the valence parameters of FeN_6 coordination octahedrons of the high-spin forms of both complexes. In **1** the average Fe−N4 bond lengths are equal to ca. 2.18 Å and the N4−Fe−N4 angles lie in the range 88.8(3)−91.4(2)° for Fe1 and 89.1(2)−91.5(2)° for Fe2. In compound **2** the average Fe−N4 bond length is equal to ca. 2.21 Å and the values of the N−Fe−N angles vary from 87.3(2)° to 94.7(2)°, indicating a significantly greater distortion of the coordination octahedron in comparison with **1**. Consequently, the complexes exhibit different magnetic properties. Complex **1** undergoes the thermally induced SCO, whereas the iron(II) ions in coordination polymer **2** remain in the high-spin state to 90 K. Probably the presence of the significantly longer Fe−N2 bonds and the greater deformation of the coordination geometry may be responsible for the stabilization of the high-spin form of **2**.

The 'polymeric approach'[47−49] to the construction of the spin crossover complexes afforded many examples of this type of material exhibiting a cooperative SCO.[50,51] On the other hand, there are also known polymeric iron(II) complexes undergoing gradual spin transition. The origin of decrease of the cooperativity is not clear, and several reasons such as flexibility of the ligand molecules,[23,24] elasticity of the coordination network,[48,52,53] or presence between polymeric subunits the competitive intermolecular interactions[54] are pointed to as responsible for such behavior. In spite of the direct connection of SCO centers, complex **1** also exhibits a gradual spin transition. The characteristic feature of this complex, at 295 K, is the presence of the disordered bridging ligand molecules, as well as ethanol molecules solvating the crystal lattice. The X-ray investigations of the HS (295 K) and LS (90 K) forms revealed a lack of significant influence of the spin transition on the intermolecular interactions. The observed compression of the crystal lattice in **1** (the volume of the unit cell decreases from 5650 $Å^3$ at 295 K to 5378 $Å^3$ at 90 K) involves the shortening of the intermolecular contacts; the number of these interactions remains unchanged. After the spin transition, the ethanol molecules remain still disordered. On the other hand, it was disclosed that the spin transition triggers the structural changes beyond the first coordination sphere of the metal ions. The HS→LS transition in **1** is accompanied by the conformational changes leading to the ordering of the ligand molecules. It means that the perturbation generated by the change of the Fe−N bond lengths is partially absorbed by the conformational labile ligand molecules. Thus, we believe that the observed gradual spin transition in **1** may be attributed to the reduction of the rigidity of the coordination network skeleton caused by the flexibility of the ligand molecules. This structural lability associated with the spin transition is reversible, and realization of the full cycle HS→LS and next LS→HS leads to the complete reconstruction of the crystal structure of the high-spin form.

Acknowledgment. The author thanks Professor Zbigniew Ciunik and Dr. Andrzej Kochel for the single-crystal X-ray data collection and the MENiS for financial support.

Supporting Information Available: X-ray crystallographic file in CIF format, complementary drawing showing the superposition of the HS and LS structures of **1**, and Table S1 containing selected intermolecular contacts. This material is available free of charge via the Internet at http://pubs.acs.org.

IC070223R

(47) Kahn, O.; Codjovi, E.; Garcia, Y.; van Koningsbruggen, P. J.; Lapayoudi, R.; Sommier, L. *Molecule-based magnetic materials*; Turnbull, M. M., Sugimoto, T., Thompson, L. K., Eds.; ACS Symposium Series 644; American Chemical Society: Washington, DC, 1996; pp 298−310.
(48) Real, J. A.; Andrés, E.; Munõz, C. M.; Julve, M.; Granier, T.; Bousseksou, A.; Varret, F. *Science* **1995**, *268*, 265−267.
(49) Kahn, O.; Martinez, C. J. *Science*, **1998**, *279*, 44−48.
(50) Real, J. A.; Gaspar, A. B.; Niel, V.; Munoz, M. C. *Coord. Chem. Rev.* **2003**, *236*, 121−141.
(51) Real, J. A.; Gaspar, A. B.; Munoz, M. C. *Dalton Trans.* **2005**, 2062−2079.
(52) Murray, K. S.; Kepert, C. J. *Top. Curr. Chem.* **2004**, *233*, 195−228.
(53) Moliner, N.; Munoz, M. C.; Letard, S.; Solans, X.; Menendez, N.; Goujon, A.; Varret, F.; Real, J. A. *Inorg. Chem.* **2000**, *39*, 5390−5393.
(54) Matouzenko, G. S.; Molnar, G.; Bréfuel, N.; Perrin, M.; Bousseksou, A.; Borshch, S. A. *Chem. Mater.* **2003**, *15*, 550−556.